HHS Public Access

Author manuscript

J Biomed Mater Res A. Author manuscript; available in PMC 2021 June 01.

Published in final edited form as:

J Biomed Mater Res A. 2021 June ; 109(6): 893–902. doi:10.1002/jbm.a.37080.

Polyanhydride nanoparticles stabilize pancreatic cancer antigen MUC4β

Luman Liu[1], **Prakash Kshirsagar**[2], **John Christiansen**[3], **Shailendra K. Gautam**[2], **Abhijit Aithal**[2], **Mansi Gulati**[2], **Sushil Kumar**[2], **Joyce C. Solheim**[4,5,6], **Surinder K. Batra**[2,4,6], **Maneesh Jain**[2,4,6], **Michael J. Wannemuehler**[3,4], **Balaji Narasimhan**[1,4]

[1]Department of Chemical and Biological Engineering, Iowa State University, Ames, Iowa

[2]Department of Biochemistry and Molecular Biology, University of Nebraska Medical Center, Omaha, Nebraska

[3]Department of Veterinary Microbiology and Preventative Medicine, Iowa State University, Ames, Iowa

[4]Nanovaccine Institute, Iowa State University, Ames, Iowa

[5]Eppley Institute for Research in Cancer and Allied Diseases, University of Nebraska Medical Center, Omaha, Nebraska

[6]Fred and Pamela Buffett Cancer Center, University of Nebraska Medical Center, Omaha, Nebraska

Abstract

Pancreatic cancer (PC) is one of the most lethal malignancies and represents an increasing and challenging threat, especially with an aging population. The identification of immunogenic PC-specific upregulated antigens and an enhanced understanding of the immunosuppressive tumor microenvironment have provided opportunities to enable the immune system to recognize cancer cells. Due to its differential upregulation and functional role in PC, the transmembrane mucin MUC4 is an attractive target for immunotherapy. In the current study we characterized the antigen stability, antigenicity and release kinetics of a MUC4β-nanovaccine to guide further optimization and, in vivo evaluation. Amphiphilic polyanhydride copolymers based on 20 mol % 1,8-bis(*p*-carboxyphenoxy)-3,6-dioxaoctane and 80 mol % 1,6-bis(*p*-carboxyphenoxy)hexane were used to synthesize nanoparticles. Structurally stable MUC4β protein was released from the particles in a sustained manner and characterized by gel electrophoresis and fluorescence spectroscopy. Modest levels of protein degradation were observed upon release. The released protein was also analyzed by MUC4β-specific monoclonal antibodies using ELISA and showed no significant loss of epitope availability. Further, mice immunized with multiple formulations of combination vaccines containing MUC4β-loaded nanoparticles generated MUC4β-specific antibody responses. These

Correspondence: Balaji Narasimhan, Department of Chemical and Biological Engineering, Iowa State University, 2035 Sweeney Hall, 618 Bissell Road, Ames, IA 50011. nbalaji@iastate.edu.

CONFLICT OF INTEREST

B. N. and M. J. W. are cofounders of ImmunoNanoMed Inc., a start-up with business interests in the development of nano-based vaccines against infectious diseases.

results indicate that polyanhydride nanoparticles are viable MUC4β vaccine carriers, laying the foundation for evaluation of this platform for PC immunotherapy.

Keywords

antigenicity; immunogenicity; MUC4; nanoparticle; pancreatic cancer; polyanhydride; protein stability

1 | INTRODUCTION

Pancreatic cancer (PC) is a devastating disease with a grim prognosis of an 8% 5-year survival rate.[1] The multifaceted challenges of PC include immune suppression, desmoplasia, early metastasis, and recurrent malignancy.[2–4] Due to early metastasis and asymptomatic nature, only 20% of patients with PC are eligible for surgical resection at the time of diagnosis.[2] Additionally, approved chemotherapy drugs, such as gemcitabine, typically only offer modest benefits to a small subset of patients.[5] Because of these challenges, effective therapies are urgently needed to improve the outcome of patients with PC. Immunotherapy, with the goal of enabling the immune system to recognize tumor associated antigens (TAAs) has emerged as a viable strategy to treat PC patients.[6]

In this context, mucins represent a class of upregulated TAAs in many adenocarcinomas, with important functions in facilitating cancer cell proliferation, migration, resistance to therapies, tumor growth, and metastasis.[7–11] During PC progression, MUC1, MUC4, MUC5AC, and MUC16 are differentially overexpressed compared to that observed in normal pancreas or during pancreatitis and exhibit altered glycosylation patterns. MUC1 has been extensively evaluated but MUC1-targeted immunotherapy has had limited success in clinical settings.[12,13] These studies have laid the foundation to study other mucins, such as MUC4, which is potentially a superior target for PC treatment. MUC4 expression is undetectable in normal pancreas and pancreatitis, but it is persistently expressed during PC progression and high expression of MUC4 is associated with poor prognosis.[9,14–19]

With the identification of neoantigens or upregulated antigens, these proteins can be purified and administered as vaccine antigens. Compared to peptide vaccines, the administration of recombinant proteins offers the advantage of exposing immune cells to multiple epitopes. However, the need for maintaining protein stability during vaccine delivery and storage becomes critical. For cancer in particular, where the antigens are normally recognized as self to some extent, prolonged time of antigen exposure and co-stimulatory molecule upregulation on antigen presenting cells (APCs) can be beneficial. In this regard, nanotechnology- and polymer-based carriers provide opportunities for sustained release of payloads and innate adjuvant capabilities, simultaneously maintaining antigen stability during encapsulation and release.[20,21]

One of the most well-studied polymer carriers is the FDA-approved, biodegradable poly(lactic-co-glycolic) acid (PLGA).[22,23] Lactic acid and glycolic acid, the degradation products of PLGA, result in acidic microenvironments, which have been implicated in protein aggregation and hydrolysis.[24,25] In contrast, polyanhydrides, which comprise

another class of biocompatible polymers, are characterized by surface erosion, tunable amphiphilic chemistry, less acidic degradation products, and controlled release of payloads.[26,27] Using two well-studied anhydride monomers, that is, 1,8-bis(*p*-carboxyphenoxy)-3,6-dioxaoctane (CPTEG) and 1,3-bis(*p*-carboxyphenoxy)hexane (CPH), the hydrophobicity of copolymers thereof can be effectively tuned to enable effective protein encapsulation while simultaneously providing an amphiphilic microenvironment to avoid deleterious protein–polymer interactions. In this regard, CPTEG:CPH copolymers of varying molar composition (50:50–20:80) have been shown to elicit differential antitumor effects and provide effective stabilization of a wide range of protein antigens.[28–33] Additionally, polyanhydride nanoparticles possess unique immune activation capabilities, leading to the induction of robust immune responses.[34,35] Additionally, this innate adjuvanticity of the particles can be combined with co-adjuvants, such as cyclic dinucleotides (CDNs), to induce pro-inflammatory immune responses[36–39]

Given the suitability of MUC4β as a PC vaccine candidate and the utility of CPTEG:CPH nanoparticles for designing subunit vaccines, we recently developed a MUC4 nanovaccine in which recombinant MUC4β subunit was encapsulated in nanoparticles composed of a 20 mol % CPTEG and 80 mol % CPH copolymer (i.e., 20:80 CPTEG:CPH) and used as carrier.[40] The MUC4 nanovaccine-activated dendritic cells as evidenced by upregulation of MHC1, MHCII, and co-stimulatory molecules, and secretion of Th1 polarizing cytokines.[40] The present study builds upon our previous work by characterizing the nanovaccine formulation in terms of protein stability, preservation of antigenicity upon release, and antigen release kinetics[30,41] in order to guide further optimization and in vivo evaluation for effective antitumor responses. We have also characterized the anti-MUC4β immune response induced by various nanovaccine formulations to delineate the synergistic effects of combining CDNs with nanoparticles. The data demonstrate the preservation of MUC4β structure and antigenicity upon encapsulation and release as well as the ability to induce anti-MUC4β antibody responses, setting the stage for further evaluation of these nanovaccines for MUC4-based PC immunotherapy.

2 | MATERIALS AND METHODS

2.1 | Materials

The chemical reagents and solvents used for monomer synthesis, polymerization, and nanoparticle (NP) synthesis were purchased from Fisher Scientific (Fairlawn, NJ) and Sigma–Aldrich (St. Louis, MO). Deuterated chloroform and dimethyl sulfoxide were used for ^{1}H nuclear magnetic resonance spectroscopy (^{1}HNMR, DXR500, Bruker, Billerica, MA). Protein concentration and stability was measured using a microbicinchoninic acid (microBCA) kit, 3,3′,5′,5′-tetramethylbenzidine (TMB) substrate kit containing soluble TMB from Thermo Scientific (Pierce, Rockford, IL), alkaline phosphatase-conjugated goat anti-mouse immunoglobulin G (H + L: Jackson ImmunoResearch, West Grove, PA), Flamingo fluorescent gel stain, and Mini-protean TGX gels from Bio-Rad (Hercules, CA). The small molecule adjuvant CDN di-GMP was purchased from Cayman Chemicals (Cat. No., 17,144, Ann Arbor, MI). Anti-MUC4α monoclonal antibodies (mAbs) 8G7 (IgG_1),

anti-MUC4β 6E8 (IgG_{2b}) and E9 (IgG_{2b}) were used for enzyme-linked immunosorbent assay (ELISA).

2.2 | Cloning strategy and protein purification

Standard PCR and molecular cloning were used to synthesize molecular clones of cDNA consisting of 733 amino acids (2199 base pairs) of human MUC4β inserted into the pET-28a vector (Novagen, Madison, WI). Expression and purification of recombinant human MUC4β protein was performed as described previously.[40,42] Briefly, the pET-28a-MUC4β plasmid was transfected into *Escherichia coli* Rosetta™ 2(DE3) competent strain, Novagen (Sigma Aldrich, Cat. No. 71400). Human MUC4β-expressing bacterial cells were harvested by centrifugation and lysed with EmulsiFlex-C3 (Avestin, Mannheim, Germany). The crude protein syrup isolated from bacterial debris was further processed to isolate insoluble inclusion bodies (i.e., Pre-AKTA pellet). The isolated pellet was suspended and dissolved in AKTA washing buffer (1× PBS, 6 M urea, 0.5% CHAPS, 20 mM imidazole, 350 mM NaCl, and 2 mM BME, pH 8.0). An isolated protein mixture was purified by AKTA Ni-NTA affinity chromatography (GE Healthcare Life Sciences) and recovered fractions were concentrated using Amicon ultra centrifugal filters (50 kDa MWCO), and dialyzed against 1× PBS and endotoxin-free water (Hyclone™, GE). Finally, MUC4β protein was passed over an endotoxin removal spin column (Fisher Scientific, Pierce Cat. No. 88282) and lyophilized overnight. The lyophilized protein (white, fluffy powder) was stored at −80°C until use.

2.3 | Polyanhydride nanoparticle synthesis and characterization

CPH and CPTEG monomers were synthesized using previously described protocols.[43] The 20:80 CPTEG:CPH copolymers were synthesized by melt polycondensation using CPH and CPTEG diacids monomers. The copolymer molecular weight (10,339 g/mol), degree of polymerization (~30), and composition (17:83) were determined by ^{1}HNMR and found to be consistent with previous studies.[43]

MUC4β protein encapsulated nanoparticles were synthesized by a solid/oil/oil anti-solvent flash precipitation method.[33,44] Briefly, 20:80 CPTEG:CPH polymer containing 2% (wt/wt) MUC4β protein was dissolved in methylene chloride at a concentration of 20 mg/ml ratio of polymer/solvent. Next, the polymer–protein solution was sonicated (30 s, 30% amplitude), and precipitated into pentane at a 1:250 volume ratio of solvent/anti-solvent. The resulting suspension was separated using vacuum filtration. Nanoparticle size and morphology were characterized by a scanning electron microscope (FEI Quanta 250, FEI, Hillsboro, OR). The average nanoparticle diameter was determined to be approximately 160 ± 28 nm using Image J (NIH, Bethesda, MD) analysis which was similar to previously observed results[33,45] (Figure 1a). Nanoparticle surface zeta potential was determined to be approximately −43.1 ± 3.1 mV using quasi-elastic light scattering (Zetasizer Nano, Malvern Instruments Ltd., Worchester, UK).

2.4 | MUC4β release from polyanhydride nanoparticles

Five milligrams of nanoparticles loaded with 2% MUC4β (wt/wt) were suspended and incubated in 350 μl phosphate-buffered saline (PBS) buffer (pH 7.4, 37°C, 102 rcf). The

particles were periodically centrifuged (15,000*g*, 5 min), all PBS buffer containing released protein was collected using a pipette and equivalent amounts of fresh buffer were added back to the tubes. To quantify the amount of protein released, the protein concentration was determined using a microBCA assay at each collection. After the final collection at day 30, the PBS buffer was replaced with 40 mM sodium hydroxide solution to accelerate polymer degradation and extract any remaining protein. The total amount of encapsulated protein and the encapsulation efficiency were calculated based on the cumulative mass of protein released and base extraction as described previously.[33]

2.5 | Analysis of MUC4β released from polyanhydride nanoparticles

MUC4β protein released after 8 hr in PBS was analyzed using sodium dodecyl sulfate polyacrylamide gel electrophoresis (SDS-PAGE) in denaturing condition. Briefly, released MUC4β protein was dried by lyophilization and redissolved into 25 μl loading buffer. The solution was boiled for 10 min prior to SDS-PAGE analysis. Approximately 10 μg of released MUC4β was loaded into Mini-Protean TGX gels (Bio-Rad) and electrophoresed (150 V, 60 min, 4°C). Gels were then incubated in fixative (40% ethanol, 10% acetic acid, 3 hr) and stained overnight with Flamingo fluorescent gel stain (Bio-Rad). The resulting gels were imaged using a Typhoon 9400 flatbed scanner (GE Healthcare).

For protein tertiary structure, the fluorescence emission levels associated with the tyrosine and tryptophan residues of the protein were measured as an indicator for the folding state. The fluorescence of the released protein (40 μg/ml) at 280 nm wavelength excitation was analyzed over the range of 300–400 nm using a SpectraMax 190 plate reader (Molecular Devices, Sunnyvale, CA). The fluorescence of both released MUC4β and unencapsulated MUC4β protein were measured and the relative peak maxima and positions were compared to assess the tertiary structure.

2.6 | Antigenicity of MUC4β released from polyanhydride nanoparticles

Epitope availability of the released MUC4β was analyzed by indirect ELISA using two anti-MUC4β-specific mAbs: 6E8 and E9. An anti-MUC4α mAb 8G7 was used as a negative control. For both unencapsulated and released MUC4β, 0.1 μg/ml protein in 100 μl/well PBS was coated in 96-well high binding microtiter plates (overnight, 4°C), after which the plates were blocked with 300 μl/well of 2.5% skim milk in nanopure water (2 hr, RT). The plates were then washed thrice with 1 × PBS supplemented with 0.05% Tween 20 (PBS-T) and incubated with 0.1 μg/ml of each anti-MUC4 mAb in PBS-T containing 1% goat serum (overnight, 4°C). After washing thrice, wells were incubated with 100 μl/well of 1:1000 diluted (in PBS-T with 1% goat serum) alkaline phosphatase-conjugated goat anti-mouse total IgG (2 hr, RT), after which the plates were washed thrice again, followed by addition of 100 μl/well of 1 mg/ml phosphatase substrate in substrate buffer (50 mM Na_2CO_3, 2 mM $MgCI_2$, pH 9.3). The colorimetric reaction was developed for 20 min and the absorbance was read at 405 nm.

2.7 | Vaccination and measurement of anti-MUC4β antibody responses

To demonstration the immunogenicity of released MUC4β, mice were immunized with MUC4β-containing nanoparticles. The STING ligand CDN was used as a co-adjuvant in

combination with the nanoparticles. Female C57BL/6 mice obtained from Charles River and Envigo (Somerset, NJ) (n = 4/group) were vaccinated with three formulations as follows (1): 20 μg CDN + 20 μg soluble MUC4β; (2) 10 μg soluble MUC4β + 10 μg MUC4β encapsulated into nanoparticles; (3) 20 μg CDN + 10 μg soluble MUC4β + 10 μg MUC4β encapsulated into nanoparticles. All formulations were delivered subcutaneously (sc) at the nape of the neck at day 0, followed by a second boost immunization at week 7. Sera before and after the second immunization were collected via saphenous vein bleeding. All animal procedures were approved by guidelines of Iowa State University Institutional Animal Care and Use Committee.

The anti-MUC4 antibody response was characterized using indirect ELISA on MUC4β-coated plates similarly as mentioned previously.40 Plates coated with MUC16CT recombinant protein were used as a negative control. Antisera were titrated using a two-fold serial dilution, starting at 1:100. Using sera of representative mice from each immunized group that had demonstrated high ELISA titers, the relative reactivity to full length human MUC4 and cleaved MUC4β were analyzed by immunoblotting for cell lysates resolved by either 2% agarose/SDS gel or 10% SDS-PAGE. Briefly, two human MUC4 expressing cell lines (H3122 and CD18/HPAF) and a MUC4 non-expressing cell line (MIA PaCA-2) were washed twice in PBS and lysed in 1× radioimmunoprecipitation assay (RIPA) buffer (50 mM Tris–HCl pH −7.5, 150 mM NaCl, 1% nonyl phenoxypolyethoxyethanol-40 (NP-40), 0.5% sodium deoxycholate, and 0.1% SDS) containing protease inhibitor mixture (Roche Diagnostics, Mannheim, Germany) and phosphatase inhibitors (1 mM NaF and 1 mM Na_3VO_4; Sigma) for 30 min on ice. Insoluble debris was removed by centrifugation (18,000*g*, 30 min, 4 C). Protein concentrations were determined using a Bio-Rad DC™ protein estimation kit (Bio-Rad). Lysates were resolved under reducing conditions by either conventional SDS-PAGE (10%) or 0.1% SDS-2% agarose gel electrophoresis as described.[46,47] Resolved proteins were transferred onto polyvinylidene difluoride membranes, blocked in 5% skim milk in PBS-T, and probed with the respective antibodies. All the antisera were used at 1:1000 dilution in 1% bovine serum albumin (BSA)/PBS. MAb 6E8 was used at 2 μg/ml in 1% BSA/PBS. After washing extensively (4×10 min, PBS-T), membranes were probed with horseradish peroxidase-conjugated goat anti-mouse secondary antibody IgG (1:3000, Thermo Fisher Scientific, Waltham, MA). Blots were washed (4×10 min, PBS-T) and processed with an ECL Chemiluminescence kit (Thermo Fisher Scientific). The signal was detected by exposing the processed blots to X-ray film (Biomax Films, Kodak, NY).

2.8 | Statistical analysis

Statistical analysis was performed using Student's *t* test and two-way ANOVA with GraphPad Prism (La Jolla, CA). *p* values less than 0.05 were considered significant.

3 | RESULTS

3.1 | Polyanhydride nanoparticles provide sustained release of MUC4β

In this work, the solid/oil/oil anti-solvent flash nanoprecipitation method was used to encapsulate MUC4β protein due to its relative hydrophobicity.[48] The MUC4β encapsulation efficiency was found to be 41% (Figure 1b). During the first 8 hr, about 30% of the

encapsulated protein was released, representing the burst effect. By day 3, 45% of encapsulated MUC4β protein was released. From day 3 onward, the protein release was steady and slow, resulting in a near zero order kinetics overall. After 30 days, about 50% of the encapsulated MUC4β was released, consistent with the surface erosion behavior of 20:80 CPTEG:CPH nanoparticles.[43]

3.2 | Released MUC4β protein is structurally stable

SDS-PAGE was used to assess the primary structure of the released MUC4β protein (Figure 2a). Analysis of both control MUC4β and released MUC4β by SDS-PAGE analysis displayed a dominant ~75 kDa band (indicated by the arrow). At the same concentration in each lane of the gel, no significant additional bands or smears were detected, indicating that the MUC4β protein was preserved from significant degradation. The slightly lighter intensity of the released MUC4β band may indicate minor protein degradation during nanoparticle synthesis and/or release.

To further analyze the structural stability of the released MUC4β protein, fluorescence spectroscopy was used to quantitatively determine tertiary folding. In a naturally folded protein, the tyrosine and tryptophan residues are often buried in a relatively hydrophobic environment, which serves to stabilize the fluorescence.[30,41] Protein unfolding exposes amino acids to a hydrophilic environment and leads to decreased fluorescence. As shown in Figure 2b, the spectra of released MUC4β were lower in fluorescence intensity compared to that of the control MUC4β protein. The decreased peak intensity at 340 nm and the red shift of released protein could represent partial unfolding of the released protein.

3.3 | MUC4β antigenicity is preserved upon release

Two recently generated MUC4β-specific mAbs (6E8 and E9) were used for antigenicity analysis. The released MUC4β protein concentration was determined by microBCA and diluted to the same concentration as unencapsulated control MUC4β. As shown in Figure 3, both anti-MUC4β mAbs successfully recognized the released MUC4β protein as well as it bound to control MUC4β. With both 6E8 and E9 antibodies, it was shown that the released protein maintained over 90% antigenic reactivity compared to control MUC4β. As a negative control, the anti-MUC4α tandem repeat (present in MUC4α)-mAb 8G7 exhibited similar reactivity to that of the no-antigen-coating control. Together, the antigenicity analysis demonstrated that despite minor loss of tertiary structure of MUC4β, the antigenic epitopes recognized by these two mAbs were still largely preserved.

3.4 | MUC4β nanovaccines induce serum antibody responses

Antisera collected from mice immunized with MUC4β nanovaccine indicated the ability to induce MUC4β-specific antibodies (Figure 4). Antibodies against MUC4β were detected by ELISA in sera from all three groups of animals that were immunized, depending upon the formulation and administration regimen. A single dose vaccination with CDN alone or 20:80 CTPEG:CPH nanoparticles alone failed to induce effective antibody responses (Figure 4a). However, combining CDNs with MUC4β-containing 20:80 CTPEG:CPH nanoparticles resulted in a demonstrable antibody response after a single dose, indicating a synergistic effect and underlining the importance of formulating antigens with the right combination of

adjuvants that balance retention of immunogenic antigen as well as mild inflammation. After a second immunization, there was a significant ($p < 0.05$) increase in MUC4β-specific antibody in sera of vaccinated animals. As a control, antibody responses to MUC16 were not detected in sera from all groups of animals (Figure 4b).

The reactivity of representative antisera to human MUC4 was characterized using western blot analysis. To resolve full length MUC4 and cleaved MUC4β, 2% SDS-agarose and 10% SDS-PAGE gels were used, respectively. In 2% SDS-agarose gel western blots, all the tested antisera recognized high molecular weight protein bands in the lysates of the MUC4 positive cells and the reactivity pattern was similar to that of anti-MUC4β mAb 6E8. Strongest reactivity was shown by antisera from animals vaccinated with the CDN + NP group, followed by NP and CDN groups, respectively, mirroring the titer seen from ELISA results. In 10% SDS-PAGE western blot, antisera from mice immunized with NP and CDN + NP groups as well as mAb 6E8 detected a ~180 kDa band selectively in MUC4 expressing NCI-H3122 lysate. The intensity of the 180 kDa band was highest in NCI-H3122 (concomitant with its high expression in 2% SDS agarose western blotting). However, no reactivity was observed with antisera from mice vaccinated with the CDN group in 10% SDS-PAGE western blot. Antisera from animals vaccinated with the CDN + NP group also showed strong recognition of 180 kDa band in CD18/HPAF lysate, whereas it was low in the antisera of animals vaccinated with the NP group. CDN group antisera and mAb 6E8 did not show detectable signal in CD18/HPAF lysate as observed in 10% SDS PAGE gel western blot. No specific binding was observed in MIA PaCa-2 lysates with any of the antibodies tested. Hence CDN + MUC4β combination nanovaccine appears to be the best inducer of anti-MUC4 immune response in mice.

4 | DISCUSSION

Mucins, including MUC4, are PC cell surface glycoproteins with important functions in promoting cancer cell growth and lubricating cell surfaces.[49] MUC4β encapsulation within polyanhydride nanoparticles may provide long-term protection against rapid phagocytic and proteolytic clearance in circulation, as shown previously for other proteins.[30–32,50] Mitigated phagocytic clearance also results in potential dose sparing, which is significant for expensive recombinant subunit vaccines, especially for manufactured mass production. Previous vaccination strategies using peptides or soluble proteins were shown to be advantageous in certain aspects, but not without challenges.[51,52] For optimal immune activation, the protein needs to be intact to present multiple epitopes, with the secondary and tertiary structures playing important roles in APC processing. The CPTEG:CPH degradation products result in a relatively neutral or only slightly acidic (6.5–7) pH microenvironment.[27] The water-free nanoparticle synthesis and the amphiphilic encapsulation environment “freezes” the protein, rendering steric inflexibility.[53] The prolonged release enables increased availability of antigen over a long duration. The data obtained herein add to the body of literature indicating the ability of 20:80 CPTEG:CPH nanoparticles as potent carriers for optimal antigen preservation.[29,50]

The MUC4β release kinetics data (Figure 1b) showed an initial burst followed by prolonged release profile. The slow near-zero order release kinetics after the initial burst is consistent

with surface erosion.[43] The initial burst of protein indicates that some protein is distributed close to the particle surface, resulting in surface porosity and allowing for rapid water penetration.[54] It has been suggested that the encapsulation and release behavior is a consequence of the polymer hydrophobicity (controlled by ratio of co-monomers), copolymer molecular weight, and surface charge, which can be tuned to the needs of different proteins.[30,55]

The SDS-PAGE analysis data in Figure 2a demonstrate the preservation of MUC4β after encapsulation and release. Despite contact with organic solvents during the fabrication process and exposure to the release environment, the recovered MUC4β was largely intact, as indicated by the similar banding pattern and intensity of the main ~75 kDa band in Figure 2a from samples before versus after nanoformulation. A slight decrease in band intensity was observed compared to the same concentration of control MUC4β, potentially indicative of slight degradation and/or aggregation. Considering that MUC4β may form inclusion bodies during purification and that it is hydrophobic, a certain degree of aggregation is not surprising.[40] It is also possible that the increased aggregation is a result of the lyophilization during protein isolation and not the encapsulation or release processes. As expected, these small changes in the released MUC4β did not reduce the epitope availability, as indicated by the antigenicity analysis shown in Figure 4.

As demonstrated by the fluorescence spectroscopy results in Figure 2b, the released MUC4β protein exhibited decreased intensity of fluorescence at the 340 nm peak absorbance and a slight red shift. The fluorescence depends on the accessibility of tyrosine and tryptophan residues to a hydrophilic solution environment, often referred to as the Stark effect, in which the exposure of tryptophan to solvent dipoles induces partial dipole reorientation.[56] The similar, yet distinct, fluorescence spectra of the released MUC4β and control MUC4β suggest a small degree of unfolding in the tertiary structure of the released MUC4β, which may impact the antigenicity and induction of MUC4β-specific antibody responses. However, the data in Figure 3, obtained with two MUC4β mAbs, indicates that there was no significant loss in antigenicity based on the epitopes recognized by the two mAbs.

Three MUC4β-containing nanovaccine formulations were administered to mice for evaluation of the MUC4β-specific antibody responses induced by the vaccines. Analysis of the antibody responses by ELISA (Figure 4) and western blot (Figure 5) showed that the MUC4β-containing nanovaccines were capable of inducing MUC4β-specific IgG. Vaccine formulations with nanoparticles induced higher antibody titers than those induced by antigen adjuvanted by CDN only. These data demonstrate the rationale for combining CDNs as a co-adjuvant with the polyanhydride nanoparticles, which is consistent with other studies.[37,57] Collectively, these studies show that encapsulation of MUC4β into nanoparticles preserves its structure and antigenicity upon release, enables sustained release of antigen (increasing the duration of antigen availability) and inclusion of CDNs as a co-adjuvant induces potent anti-MUC4β immune responses. Our previous work with these nanovaccine formulations indicated the ability of these formulations to induce robust T cell immunity[50,58] and our ongoing work is focused on characterization of T cell cytotoxicity after MUC4β nanovaccine immunization.

5 | CONCLUSIONS

In summary, our studies show that the amphiphilic polyanhydride copolymers are suitable for MUC4β encapsulation. In addition, stable MUC4β is released from these nanoparticles, as evidenced by the maintenance of its structural integrity and antigenicity. The vaccination of mice with MUC4β nanovaccines verified the immunogenicity of the released MUC4. In summary, all these studies lay a foundation for evaluating the potential use of polyanhydride-based nanovaccine for PC immunotherapy.

ACKNOWLEDGMENTS

This work was supported by the National Institute of Health (U01 CA213862) and the Iowa State University Nanovaccine Institute. B. N. is grateful to the Vlasta Klima Balloun Faculty Chair.

Funding information

National Cancer Institute, Grant/Award Number: U01 CA213862

REFERENCES

1. Siegel RL, Miller KD, Jemal A. Cancer statistics, 2016. CA Cancer J Clin. 2016;66:7–30. [PubMed: 26742998]
2. Oberstein PE, Olive KP. Pancreatic cancer: why is it so hard to treat? Therap Adv Gastroenterol. 2013;6(4):321–337.
3. Sideras K, Braat H, Kwekkeboom J, van Eijck CH, Peppelenbosch MP, Sleijfer S, Bruno M. Role of the immune system in pancreatic cancer progression and immune modulating treatment strategies. Cancer Treat Rev; 2014;40:513–22. [PubMed: 24315741]
4. Erkan M, Hausmann S, Michalski CW, et al. The role of stroma in pancreatic cancer: diagnostic and therapeutic implications [Internet. Nat Rev Gastroenterol Hepatol. 2012;9:454–467. [PubMed: 22710569]
5. Gresham GK, Wells GA, Gill S, Cameron C, Jonker DJ. Chemotherapy regimens for advanced pancreatic cancer: a systematic review and network meta-analysis. BMC Cancer. 2014;14:1–13. [PubMed: 24383403]
6. Banerjee K, Kumar S, Ross KA, et al. Emerging trends in the immunotherapy of pancreatic cancer. Cancer Lett. 2018;417:35–46. [PubMed: 29242097]
7. Torres MP, Chakraborty S, Souchek J, Batra SK. Mucin-based targeted pancreatic cancer therapy. Curr Pharm Des. 2012;18:2472–2481. [PubMed: 22372499]
8. Remmers N, Anderson JM, Linde EM, et al. Aberrant expression of mucin core proteins and O-linked glycans associated with progression of pancreatic cancer. Clin Cancer Res. 2013;19:1981–1993. [PubMed: 23446997]
9. Kaur S, Kumar S, Momi N, Sasson AR, Batra SK. Mucins in pancreatic cancer and its microenvironment. Nat Rev Gastroenterol Hepatol. 2013;10:607–620. Available from:. 10.1038/nrgastro.2013.120. [PubMed: 23856888]
10. Bhatia R, Gautam SK, Cannon A, et al. Cancer-associated mucins: role in immune modulation and metastasis. Cancer Metastasis Rev. 2019; 38:223–236. [PubMed: 30618016]
11. Gautam SK, Kumar S, Cannon A, et al. MUC4 mucin-a therapeutic target for pancreatic ductal adenocarcinoma. Expert Opin Ther Targets. 2017;21(7):657–669. [PubMed: 28460571]
12. Koido S, Homma S, Takahara A, et al. Current immunotherapeutic approaches in pancreatic cancer. Clin Dev Immunol. 2011;2011:1–15.
13. Plate J Clinical trials of vaccines for immunotherapy in pancreatic cancer. Expert Rev Vaccines. 2011;10:825–836. [PubMed: 21692703]
14. Swartz MJ, Batra SK, Varshney GC, et al. MUC4 expression increases progressively in pancreatic intraepithelial neoplasia. Am J Clin Pathol. 2002;117:791–796. [PubMed: 12090430]

15. Saitou M, Goto M, Horinouchi M, et al. MUC4 expression is a novel prognostic factor in patients with invasive ductal carcinoma of the pancreas. J Clin Pathol. 2005;58:845–852. [PubMed: 16049287]
16. Hinoda Y, Ikematsu Y, Horinochi M, et al. Increased expression of MUC1 in advanced pancreatic cancer. J Gastroenterol. 2003;38:1162–1166. [PubMed: 14714254]
17. Horn A, Chakraborty S, Dey P, et al. Immunocytochemistry for MUC4 and MUC16 is a useful adjunct in the diagnosis of pancreatic adenocarcinoma on fine-needle aspiration cytology. Arch Pathol Lab Med. 2013;137:546–551. [PubMed: 23544943]
18. Westgaard A, Schjølberg AR, Cvancarova M, Eide TJ, Clausen OPF, Gladhaug IP. Differentiation markers in pancreatic head adenocarcinomas: MUC1 and MUC4 expression indicates poor prognosis in pancreatobiliary differentiated tumours. Histopathology. 2009;54: 337–347. [PubMed: 19236510]
19. Chaturvedi P, Singh AP, Batra SK. Structure, evolution, and biology of the MUC4 mucin. FASEB J. 2007;22:966–981. [PubMed: 18024835]
20. Kamaly N, Yameen B, Wu J, Farokhzad OC. Degradable controlled-release polymers and polymeric nanoparticles: mechanisms of controlling drug release. Chem Rev. 2016;116:2602–2663. [PubMed: 26854975]
21. Narasimhan B, Goodman JT, Vela Ramirez JE. Rational design of targeted next-generation carriers for drug and vaccine delivery. Annu Rev Biomed Eng. 2016;18:25–49. [PubMed: 26789697]
22. Danhier F, Ansorena E, Silva JM, Coco R, Le Breton A, Préat V. PLGA-based nanoparticles: an overview of biomedical applications. J Control Release. 2012;161:505–522. [PubMed: 22353619]
23. Bobo D, Robinson KJ, Islam J, Thurecht KJ, Corrie SR. Nanoparticle-based medicines: a review of FDA-approved materials and clinical trials to date. Pharm Res. 2016;33:2373–2387. [PubMed: 27299311]
24. Duque L, Körber M, Bodmeier R. Improving release completeness from PLGA-based implants for the acid-labile model protein ovalbumin. Int J Pharm. 2018;538:139–146. [PubMed: 29355654]
25. Han R, Zhu J, Yang X, Xu H. Surface modification of poly(D, L -lactic-co-glycolic acid) nanoparticles with protamine enhanced cross-presentation of encapsulated ovalbumin by bone marrow-derived dendritic cells. J Biomed Mater Res A. 2011;96:142–149. [PubMed: 21105162]
26. Determan AS, Graham JR, Pfeiffer KA, Narasimhan B. The role of microsphere fabrication methods on the stability and release kinetics of ovalbumin encapsulated in polyanhydride microspheres. J Microencapsul. 2006;23:832–843. [PubMed: 17390625]
27. Torres MP, Determan AS, Anderson GL, Mallapragada SK, Narasimhan B. Amphiphilic polyanhydrides for protein stabilization and release. Biomaterials. 2007;28:108–116. [PubMed: 16965812]
28. Petersen LK, Xue L, Wannemuehler MJ, Rajan K, Narasimhan B. The simultaneous effect of polymer chemistry and device geometry on the in vitro activation of murine dendritic cells. Biomaterials. 2009;30: 5131–5142. [PubMed: 19539989]
29. Wafa EI, Geary SM, Goodman JT, Narasimhan B, Salem AK. The effect of polyanhydride chemistry in particle-based cancer vaccines on the magnitude of the anti-tumor immune response. Acta Biomater. 2017;50:417–427. [PubMed: 28063991]
30. Ross KA, Loyd H, Wu W, et al. Structural and antigenic stability of H5N1 hemagglutinin trimer upon release from polyanhydride nanoparticles. J Biomed Mater Res A. 2014;102:4161–4168. [PubMed: 24443139]
31. Vela Ramirez JE, Roychoudhury R, Habte HH, Cho MW, Pohl NLB, Narasimhan B. Carbohydrate-functionalized nanovaccines preserve HIV-1 antigen stability and activate antigen presenting cells. J Biomater Sci Polym Ed. 2014;25:1387–1406. [PubMed: 25068589]
32. Haughney SL, Petersen LK, Schoofs AD, et al. Retention of structure, antigenicity, and biological function of pneumococcal surface protein a (PspA) released from polyanhydride nanoparticles. Acta Biomater. 2013;9:8262–8271. [PubMed: 23774257]
33. Petersen LK, Phanse Y, Ramer-Tait AE, Wannemuehler MJ, Narasimhan B. Amphiphilic polyanhydride nanoparticles stabilize *Bacillus anthracis* protective antigen. Mol Pharm. 2012;9:874–882. [PubMed: 22380593]

34. Ulery BD, Petersen LK, Phanse Y, et al. Rational design of pathogen-mimicking amphiphilic materials as nanoadjuvants. Sci Rep. 2011;1: 1–9. [PubMed: 22355520]
35. Petersen LK, Ramer-Tait AE, Broderick SR, et al. Activation of innate immune responses in a pathogen-mimicking manner by amphiphilic polyanhydride nanoparticle adjuvants. Biomaterials. 2011;32:6815–6822. [PubMed: 21703679]
36. Joshi VB, Geary SM, Carrillo-Conde BR, Narasimhan B, Salem AK. Characterizing the antitumor response in mice treated with antigen-loaded polyanhydride microparticles. Acta Biomater. 2013;9:5583–5589. [PubMed: 23153760]
37. Ross K, Senapati S, Alley J, et al. Single dose combination nanovaccine provides protection against influenza A virus in young and aged mice. Biomater Sci. 2019;7:809–821. [PubMed: 30663733]
38. Wafa EI, Geary SM, Ross KA, Goodman JT, Narasimhan B, Salem AK. Pentaerythritol-based lipid A bolsters the antitumor efficacy of a polyanhydride particle-based cancer vaccine. Nanomedicine. 2019;21: 102055. [PubMed: 31319179]
39. Schaut RG, Brewer MT, Hostetter JM, et al. A single dose polyanhydride-based vaccine platform promotes and maintains anti-GnRH antibody titers. Vaccine. 2018;36:1016–1023. [PubMed: 29413092]
40. Banerjee K, Gautam SK, Kshirsagar P, et al. Amphiphilic polyanhydride-based recombinant MUC4β-nanovaccine activates dendritic cells. Genes Cancer. 2019;10:52–62. [PubMed: 31258832]
41. Carrillo-Conde B, Schiltz E, Yu J, et al. Encapsulation into amphiphilic polyanhydride microparticles stabilizes Yersinia pestis antigens. Acta Biomater. 2010;6:3110–3119. [PubMed: 20123135]
42. Aithal A, Junker WM, Kshirsagar P, et al. Development and characterization of carboxy-terminus specific monoclonal antibodies for understanding MUC16 cleavage in human ovarian cancer. PLoS One. 2018; 13:1–18.
43. Torres MP, Vogel BM, Narasimhan B, Mallapragada SK. Synthesis and characterization of novel polyanhydrides with tailored erosion mechanisms. J Biomed Mater Res A. 2006;76:102–110. [PubMed: 16138330]
44. Kipper MJ, Shen E, Determan A, Narasimhan B. Design of an injectable system based on bioerodible polyanhydride microspheres for sustained drug delivery. Biomaterials. 2002;23:4405–4412. [PubMed: 12219831]
45. Ulery BD, Kumar D, Ramer-Tait AE, Metzger DW, Wannemuehler MJ, Narasimhan B. Design of a protective single-dose intranasal nanoparticle-based vaccine platform for respiratory infectious diseases. PLoS One. 2011;6:1–8.
46. Moniaux N, Varshney GC, Chauhan SC, et al. Generation and characterization of anti-MUC4 monoclonal antibodies reactive with normal and cancer cells in humans. J Histochem Cytochem. 2004;52: 253–261. [PubMed: 14729877]
47. Jain M, Venkatraman G, Moniaux N, et al. Monoclonal antibodies recognizing the non-tandem repeat regions of the human mucin MUC4 in pancreatic cancer. PLoS One. 2011;6:2–9.
48. D'Addio SM, Prud'homme RK. Controlling drug nanoparticle formation by rapid precipitation. Adv Drug Deliv Rev. 2011;63: 417–426. [PubMed: 21565233]
49. Rachagani S, Macha MA, Ponnusamy MP, et al. MUC4 potentiates invasion and metastasis of pancreatic cancer cells through stabilization of fibroblast growth factor receptor 1. Carcinogenesis. 2012;33: 1953–1964. [PubMed: 22791819]
50. Huntimer LM, Ross KA, Darling RJ, et al. Polyanhydride nanovaccine platform enhances antigen-specific cytotoxic T cell responses. Dent Tech. 2014;02:171–175.
51. Hailemichael Y, Dai Z, Jaffarzad N, et al. Persistent antigen at vaccination sites induces tumor-specific CD8+ T cell sequestration, dysfunction and deletion. Nat Med. 2013;19:465–472. [PubMed: 23455713]
52. Fan Y, Moon JJ. Nanoparticle drug delivery systems designed to improve cancer vaccines and immunotherapy. Vaccine. 2015;3: 662–685.
53. Klibanov AM. Improving enzymes by using them in organic solvents in organic solvents. Nature. 2001;409:241–246. [PubMed: 11196652]

54. Göpferich A, Tessmar J. Polyanhydride degradation and erosion. Adv Drug Deliv Rev. 2002;54:911–931. [PubMed: 12384315]

55. Zhao H, Lin ZY, Yildirimer L, Dhinakar A, Zhao X, Wu J. Polymer-based nanoparticles for protein delivery: design, strategies and applications. J Mater Chem B. 2016;4(23), 4060–4071. [PubMed: 32264607]

56. Vivian JT, Callis PR. Mechanisms of tryptophan fluorescence shifts in proteins. Biophys J. 2001;80:2093–2109. [PubMed: 11325713]

57. Wilson DR, Sen R, Sunshine JC, Pardoll DM, Green JJ, Kim YJ. Biodegradable STING agonist nanoparticles for enhanced cancer immunotherapy. Nanomedicine. 2018;14:237–246. [PubMed: 29127039]

58. Zacharias ZR, Ross KA, Hornick EE, et al. Polyanhydride nanovaccine induces robust pulmonary B and T cell immunity and confers protection against homologous and heterologous influenza A virus infections. Front Immunol. 2018;9:1953. [PubMed: 30233573]

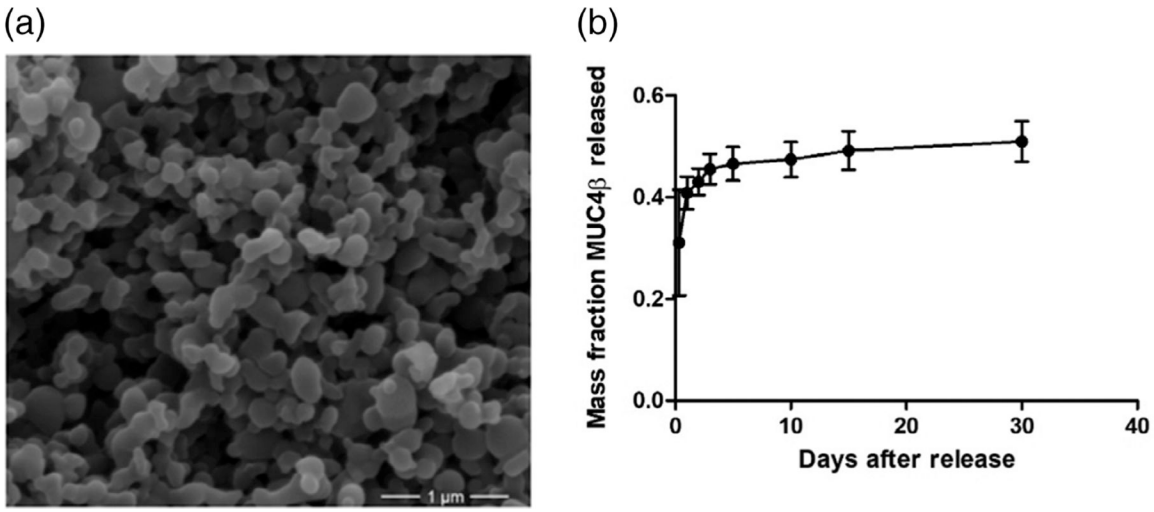

FIGURE 1.

Nanoparticle synthesis and sustained release of MUC4β antigen. (a) Scanning electron microscopy image showing representative 2% MUC4β-loaded 20:80 CPTEG:CPH polyanhydride nanoparticles. Scale bar: 1 μm. (b) Release profile of MUC4β from 20:80 CPTEG:CPH polyanhydride nanoparticles for 30 days. Error bars represent *SD*. Three independent replicates were analyzed in the release studies. CPH, 1,3-bis (*p*-carboxyphenoxy)hexane; CPTEG, 1,8-bis(*p*-carboxyphenoxy)-3,6-dioxaoctane

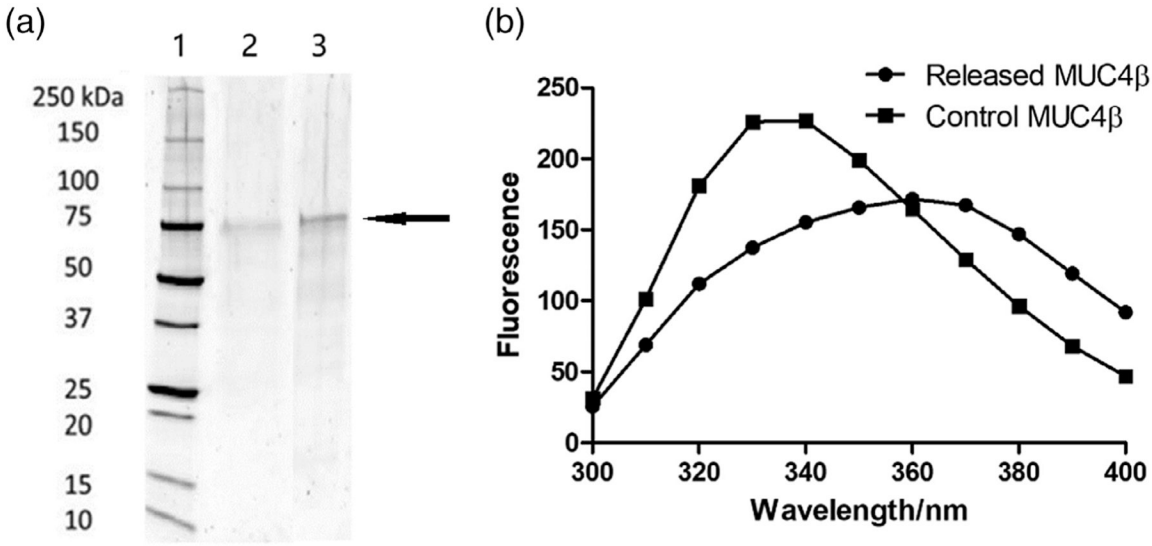

FIGURE 2.

Analysis of MUC4β structural stability. (a) SDS-PAGE of MUC4β released from nanoparticles. Lanes represent (1) molecular weight standard ladder; (2) released MUC4β; and (3) control MUC4β with 10 μg in each lane. The arrow indicates the location of the main MUC4β protein band. (b) Fluorescence spectroscopy of MUC4β released from nanoparticles. SDS-PAGE, sodium dodecyl sulfate polyacrylamide gel electrophoresis

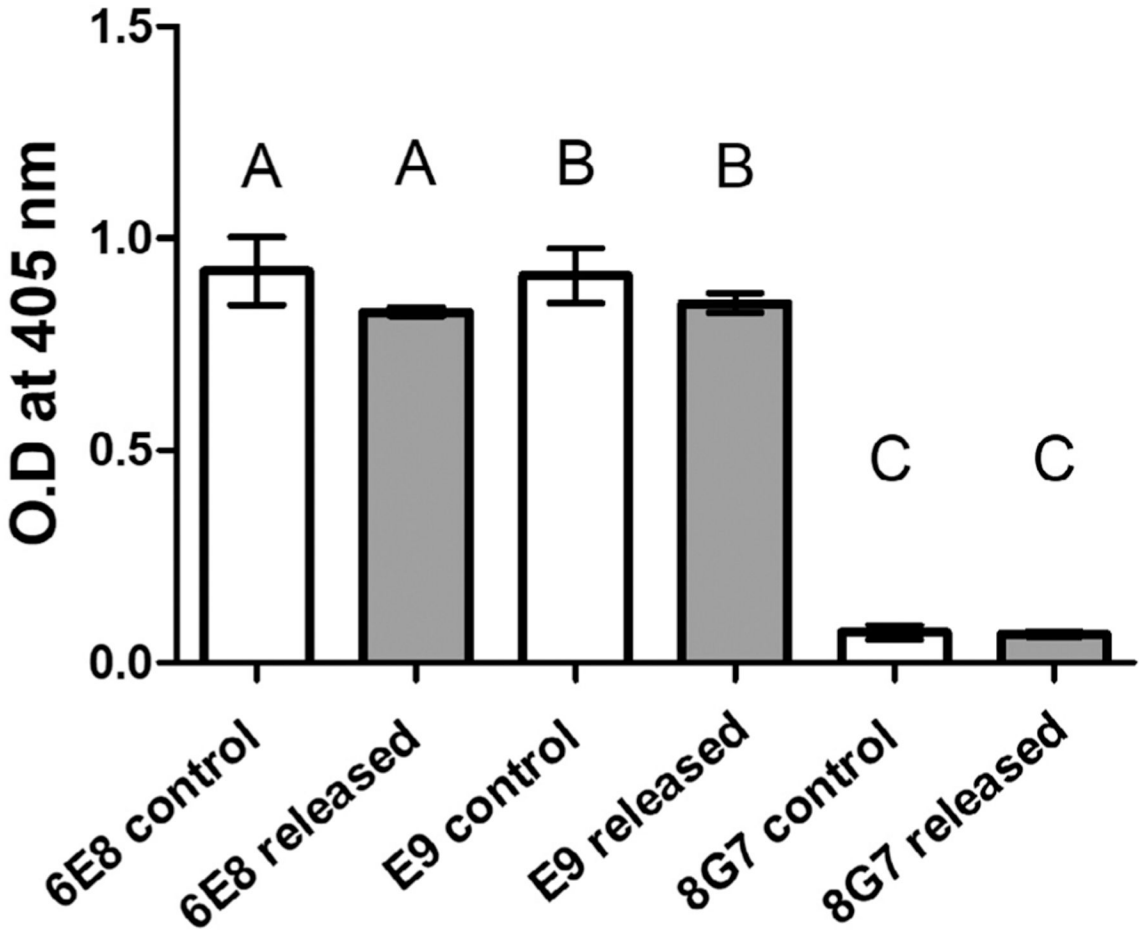

FIGURE 3.

MUC4β antigen epitope availability (represented as an OD@405 nm) upon recognition by distinct anti-MUC4β mAbs. Indirect ELISA was used to assess the reactivity of each mAb against MUC4β released from the nanoparticles. No significant differences relative to the control MUC4β (at the same MUC4β coating concentration) were observed with mAbs 6E8 and E9. Reactivity of anti-MUC4α mAb 8G7 was not significantly different from the no-antigen-coating control. Error bars represent *SEM*. No significance was observed in comparison to the corresponding control (using $p < 0.05$). mAbs, monoclonal antibodies

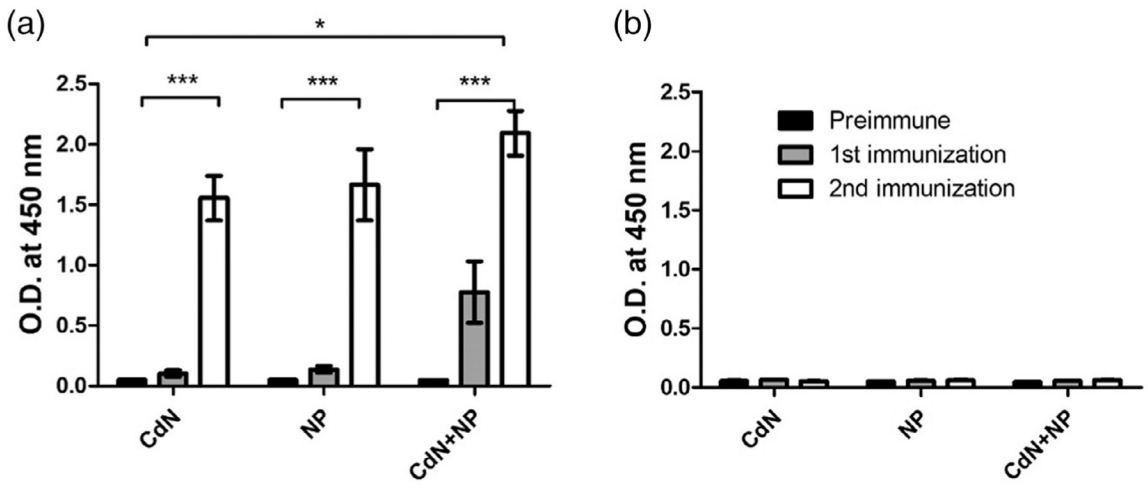

FIGURE 4.

Anti-MUC4 immune response from sera of mice vaccinated with three MUC4β-based vaccine formulations. (a) Indirect ELISA using MUC4β coated plates. (b) Indirect ELISA using MUC16-coated plates. Significant differences were observed depending on formulation and regimen. Reactivity of CDN + NP combination formulations was significantly higher than that provided by either CDN or NP alone. Reactivity after second immunization is significantly higher than that of the pre-immune control and after single immunization. For both MUC4β- and MUC16-coated plates, OD values at 1:6400 dilution were used to generate the plots. Data were not normalized. Error bars represent *SEM*. * indicates statistical significance ($p < 0.05$) between different vaccine formulations. *** indicates statistical significance ($p < 0.05$) between from secondary immunization to primary immunization and unimmunized group. CDN, cyclic dinucleotide

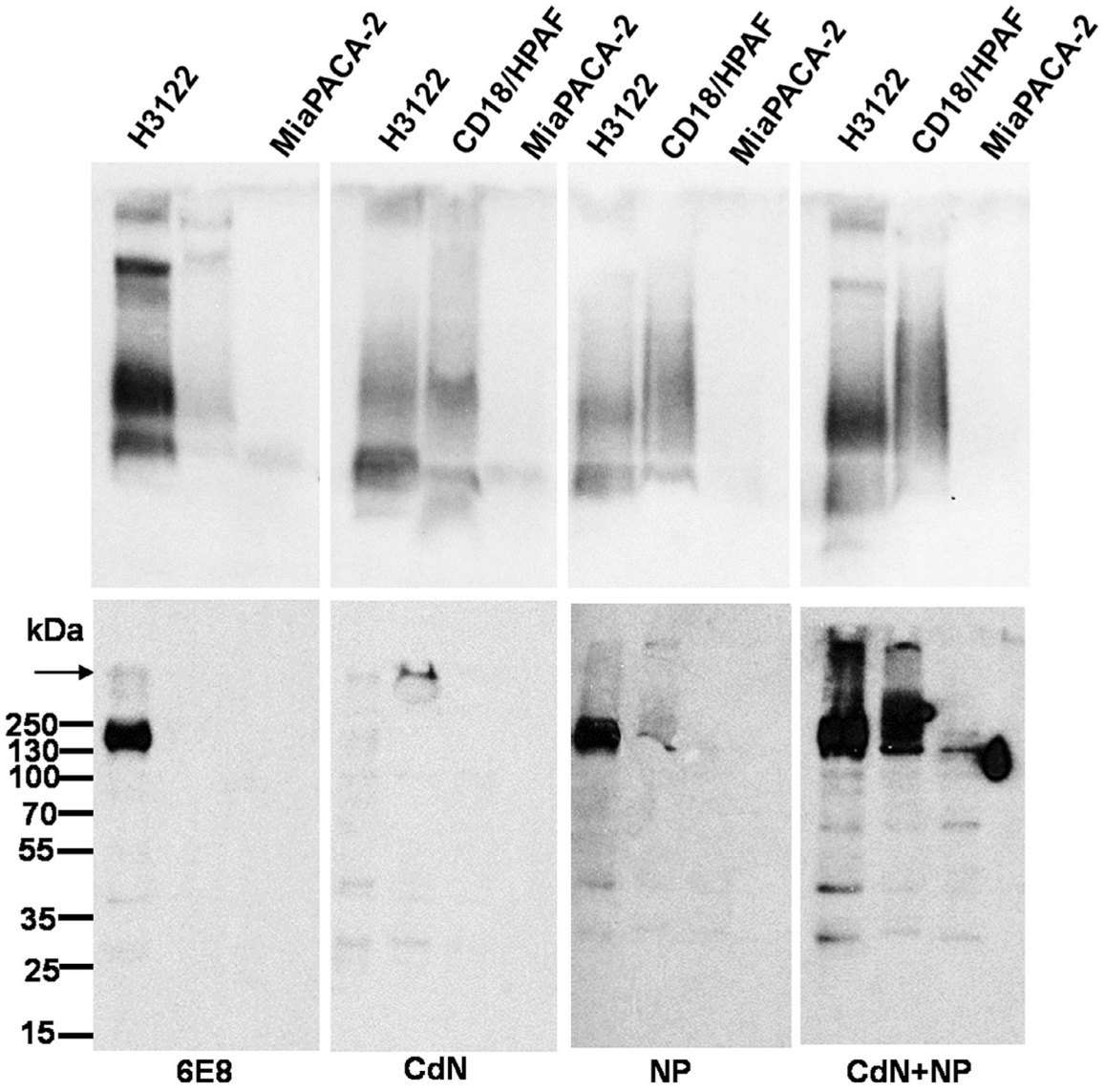

FIGURE 5.

Relative reactivities of different MUC4β nanovaccine elicited antisera to full length human MUC4 and cleaved MUC4β fragment. Western blotting analysis of protein lysates (80 μg) from three different cell lines resolved either on 2% SDS-agarose gels (upper panel) or 10% SDS PAGE gels (lower panel) and passively transferred to the PVDF membrane and probed with the sera from mice immunized with the indicated formulations. Anti-MUC4β mAb 6E8 was used as a positive control. The arrow indicates the interface of stacking and resolving gels. The molecular weight markers are indicated on the left. PVDF, polyvinylidene difluoride; SDS-PAGE, sodium dodecyl sulfate polyacrylamide gel electrophoresis